International Journal of Nanoelectronics and Materials
Volume 15 (Special Issue) March 2022 [495-504]

Effects of Rotary Ultrasonic Assisted Drilling Parameter for Carbon Fiber Reinforce Plastic Laminate Composites

M. S. A. Aziz[2], R. Izamshah[1*], M. S. Yob[1], M. S. Kasim[1], S. A. Sundi[3] and R. Zamri[2] and [4] R. S. A. Abdullah

[1]Advanced Manufacturing Centre (AMC), Universiti Teknikal Malaysia Melaka,
Hang Tuah Jaya, 76100 Durian Tunggal, Melaka, Malaysia
[2]Fakulti Kejuruteraan Pembuatan, Universiti Teknikal Malaysia Melaka,
Hang Tuah Jaya, 76100 Durian Tunggal, Melaka, Malaysia
[3]Fakulti Teknologi Kejuruteraan Mekanikal dan Pembuatan, Universiti Teknikal Malaysia Melaka,
Hang Tuah Jaya, 76100 Durian Tunggal, Melaka, Malaysia
[4]School of Information Technology and Electrical Engineering, The University of Queensland,
Brisbane, Queensland 4072, Australia

ABSTRACT

The unique properties of Carbon Fiber Reinforced Plastic (CFRP) laminate composite such as lightweight, tailored properties, high strength, and design flexibility has made it as an alternative material for aerospace components. Owing to the disparate properties of plies across the part thickness has create challenges for the manufacturer to achieve high quality holes through conventional drilling technique. Some of the challenges includes delamination, matrix cracking, uncut fiber and rough surface which require additional finishing step for de-burring. To solve with the issues, rotary ultrasonic assisted drilling (RUAD) process is proposed. Hence, this project aims to investigate the ultrasonic assisted drilling parameter for effectively drilling CFRP material. Four main drilling parameters to be evaluate experimentally (rotational speed, feed rate, vibration amplitude and frequency) towards the hole performances namely hole accuracy for entry and exit surface areas. Based on the conducted investigation, it shows that vibration amplitude and speed have significant effect for the hole entry surface error while feed rate and speed have significant effect for the hole exit surface error. The outcomes from this research can be used as an input for the decision making process for improving the hole accuracy in drilling CFRP laminate material.

Keywords: Rotary ultrasonic assisted drilling, Carbon Fiber Reinforced Plastic (CFRP), Machining performance

1. INTRODUCTION

The use of carbon fiber reinforced plastic (CFRP) in aerospace application have ultimately increased over the last decade due to its design flexibility and tailored properties. CFRP material offers an excellent strength together with low density, low coefficient of thermal expansion, excellent in fatigue and high corrosion resistance which required for the aero-structure component [1]. In general, it is compulsory to perform a post-machining operation such as drilling of the CFRP parts for assembly and joining purposed [2]. However, drilling with conventional methods poses several challenges including delamination, matrix cracking, uncut fiber and rough surface which require additional finishing step for de-burring.

Based on the challenges arise with the current conventional drilling hole making process, new techniques are necessitating. Rotary ultrasonically assisted drilling (RUAD) is a hybrid machining process that incorporates between conventional drilling and high-frequency superimposed vibration amplitude transmit axially to the drill bit tip.

*izamshah@utem.edu.my

Based on the literature, ultrasonic assisted drilling has demonstrated promising results to improve the machining processes including milling [3-6], turning [7-9], grinding [10-12] and drilling [13-15] for various material such as super alloys, tool steel, ceramic, composite and glass. The reported improvement includes reduction in cutting force, burr formation, surface roughness, cutting temperature, hole error and increase material removal rate.

In this paper, effects of four main RUAD parameter (rotational speed, feed rate, vibration amplitude and frequency) towards the hole performances namely hole accuracy and surface roughness will be evaluating experimentally prior to the optimization process.

2. DRILLING INDUCED DAMAGES IN CFRP LAMINATE

Generally, damage during the drilling process of CFRP laminate can occur at both entry and exit hole. At the hole entry, damage in ply delamination occurred through three phases step process. In the first phase, the fibers on the surface layer was break/cut by the drill chisel cutting edges and continue to break by the twisted edge gaps that ejected both the fiber chips and matrix fragments at the second phase. Finally, the upward force peeled the uncut fibers up from the material surface. On the other hand, the damage at the hole exit was mainly caused by the bending deformation of the uncut laminate due to the significant thrust force in which as the downward thrust force exceeded the fiber-matrix bonding strength, the inter-laminar de-bonding appeared and delamination happened at the hole exit. Figure 1 and 2 show the mechanic of drilling induced damages in CFRP laminate.

Based on this, it can be observed that the relationship between the thrust force and the critical de-bonding force would directly relate with the damage induced. Therefore, controlling and reducing the cutting force during the drilling process are essential for achieving a quality hole. One of the possible technique to reduce the cutting force are by introducing the axial movement such as in ultrasonic assisted drilling technique.

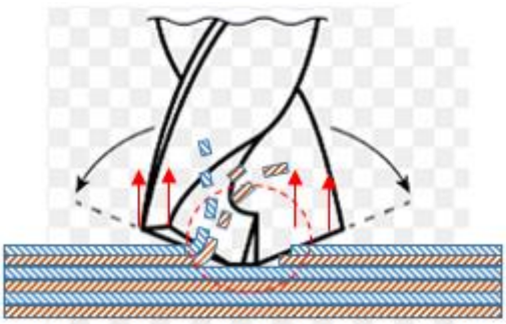

Figure 1. Mechanic of peel-up delamination at the hole entrance.

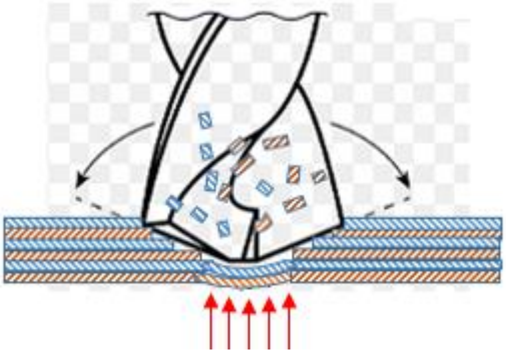

Figure 2. Push-out delamination at the exit.

3. MATERIAL AND METHOD

3.1 Carbon Fiber Reinforced Plastic (CFRP)

The CFRP panel measured 3.25 mm in thickness and the type of fabric was unidirectional (UD). Total number of plies was 28 in total. There were two thin 0.08 mm layers of glass/epoxy woven fabrics used at the top and bottom of the CFRP to protect the outer surfaces of the panel. The 26 unidirectional plies were made of carbon/epoxy preparation manufactured by Hexcel Composite Company. The stacking sequence was [45/135/90/90/0/90/0/90/0/135/45/45/135/135/45/45/135/0/90/0/90/0/90/90/135/45]. The nominal fiber volume fraction is 60 %. Table 1 illustrates the overall specification of CFRP material used in this work

Table 1 Carbon Fiber Reinforce Plastic Specification

Composite Composition	No of Ply	Area Density (g/m^3)	Type of Fiber	CPT/Ply
Carbon	26	203	Unidirectional	0.125
Glass	2	107	Woven	0.08
Total thickness (mm)				3.25

3.2 Experimental Setup

The drilling experiment was conducted using a 3 axis CNC milling machine. A dedicated ultrasonic tooling system was designed and developed to suit with the machine spindle specification to perform the RUAD process. The ultrasonic tooling system capable to transmit ultrasonic frequency from the generator oscillating from 20 kHz to 27 kHz with maximum of 5 µm amplitude. The developed RUAD system and CFRP workpiece glass arrangement are illustrate in Figure 3 below. In addition, special design jig and fixturing were fabricated to minimize the present of chatter. The design of the work holding device need to be rigid to cater the compressive stress occur during the RUAD process in both entry and exit surfaces. A standard two-flute solid carbide twist drill with a diameter of 6 mm having a point and helix angles of 140^o and 28^o, respectively, was used for all experimental studies.

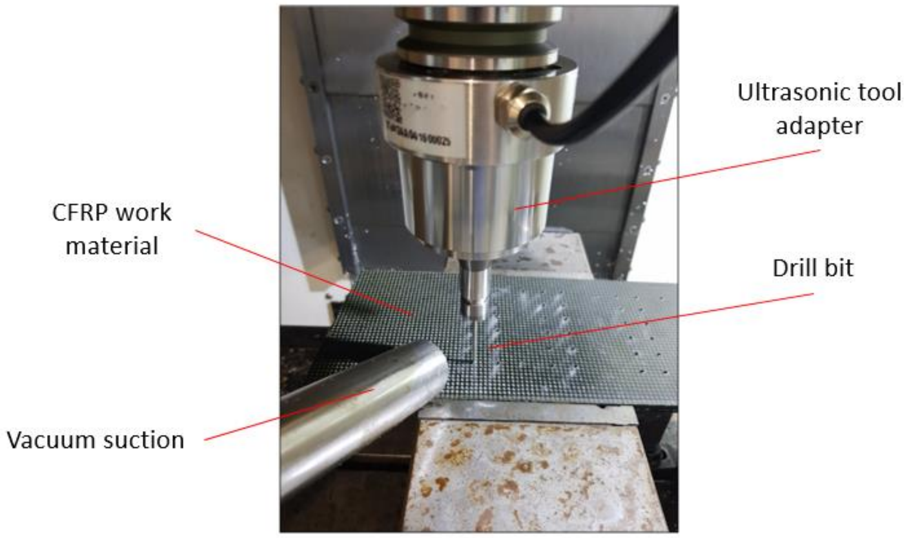

Figure 3. Experimental setup.

Central Composite Design matrix of Response Surface Methodology (RSM) technique was used as the Design of Experiment (DoE) to evaluate the RUAD parameters input to the output responses. Totals of 30 experimental runs were perform consist of independent variables and levels namely; spindle speed (A), feed rate (B), ultrasonic frequency (C) and vibration amplitude(D) as explained in Table 2. The upper and lower limit value for the input variables were based from cutting tool's manufacturer recommendations and from the literature [2]. Optical microscope was used to captured the drilled holes images for the analysis. Subsequently, the image will be process by the ImageJ® software for measuring the chipping area at both entry and exit surface. Figure 7 illustrated the step taken for calculating the total chipping area i.e. entry and exit surfaces errors. To ensure the accuracy of the reading, the measurements were done five times.

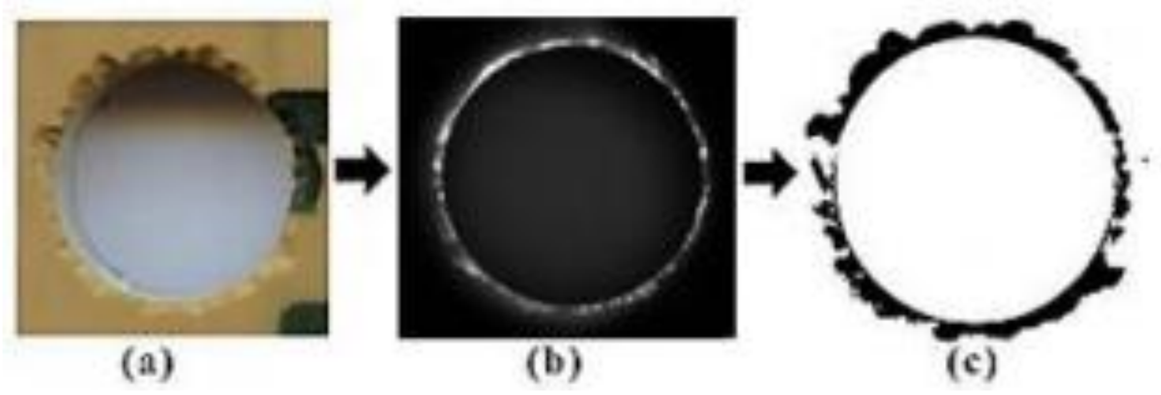

Figure 4. Hole error measurement using image processing to determine the burr area (a) captured hole image, (b) intermediate processed image and (c) final processed image.

Table 2 Experimental Runs

Run	A: Speed	B: Feed Rate	C: Freq.	D: Amp.	Run	A: Speed	B: Feed rate	C: Freq.	D: Amp.
	(rpm)	(mm/tooth)	(KHz)	(μm)		(rpm)	(mm/tooth)	(KHz)	(μm)
1	1500	0.05	20	1	16	2500	0.1	27	3
2	2500	0.05	20	1	17	1000	0.075	23.5	2
3	1500	0.1	20	1	18	3000	0.075	23.5	2
4	2500	0.1	20	1	19	2000	0.025	23.5	2
5	1500	0.05	27	1	20	2000	0.125	23.5	2
6	2500	0.05	27	1	21	2000	0.075	16.5	2
7	1500	0.1	27	1	22	2000	0.075	30.5	2
8	2500	0.1	27	1	23	2000	0.075	23.5	0
9	1500	0.05	20	3	24	2000	0.075	23.5	4
10	2500	0.05	20	3	25	2000	0.075	23.5	2
11	1500	0.1	20	3	26	2000	0.075	23.5	2
12	2500	0.1	20	3	27	2000	0.075	23.5	2
13	1500	0.05	27	3	28	2000	0.075	23.5	2
14	2500	0.05	27	3	29	2000	0.075	23.5	2
15	1500	0.1	27	3	30	2000	0.075	23.5	2

4. RESULTS AND DISCUSSION

Table 3 and Figure 5 tabulated the holes' performances for both entry and exit surfaces. The observed hole error area value for both entry and exit surfaces varied between 0.032 mm^2 to 0.699 mm^2 and 0.099 mm^2 to 0.845 mm^2 respectively. The variations on the observed values indicate that the RUAD drilling parameters has significant effects on the hole's quality. Figure 6 shows the samples for the minimum and maximum burr area formation. In addition, it was found that the holes at the exit area surface exhibits worse burr formation as compared to the entry holes.

Table 3 Experimental Results

Run	Hole Entry Error (mm^2)	Hole Exit Error (mm^2)	Run	Hole Entry Error (mm^2)	Hole Exit Error (mm^2)
1	0.699	0.418	16	0.332	0.494
2	0.27	0.685	17	0.224	0.171
3	0.415	0.745	18	0.433	0.099
4	0.409	0.586	19	0.098	0.325
5	0.499	0.199	20	0.137	0.767
6	0.198	0.282	21	0.221	0.471
7	0.481	0.845	22	0.082	0.621
8	0.465	0.758	23	0.242	0.431
9	0.118	0.509	24	0.032	0.56

10	0.177	0.504	25	0.079	0.521
11	0.156	0.651	26	0.09	0.574
12	0.22	0.745	27	0.082	0.577
13	0.132	0.589	28	0.087	0.55
14	0.298	0.382	29	0.078	0.62
15	0.098	0.669	30	0.092	0.54

4.1 Effects of RUAD Parameters on Hole Entry Surface Error

Statistical ANOVA of surface error areas (Table 4) was performed to further investigated the effects of RUAD parameters. Based on the ANOVA, a quadratic model was selected to exemplify the cutting parameters effects towards the entry burr surface areas. From the analysis, it indicated that vibration amplitude and spindle speed were the most significant factors that affect the hole entry accuracy. The results revealed that, the presence of ultrasonic vibration acts as an additional axial sawing/cutting action that effectively break the fiber.

Figure 7 shows a 3d response surface plot on the entry burr area with regards to the speed and vibration amplitude. Based on the graph, it shows that the minimum hole error surface occurred at the region when vibration amplitude is high and spindle speed is medium.

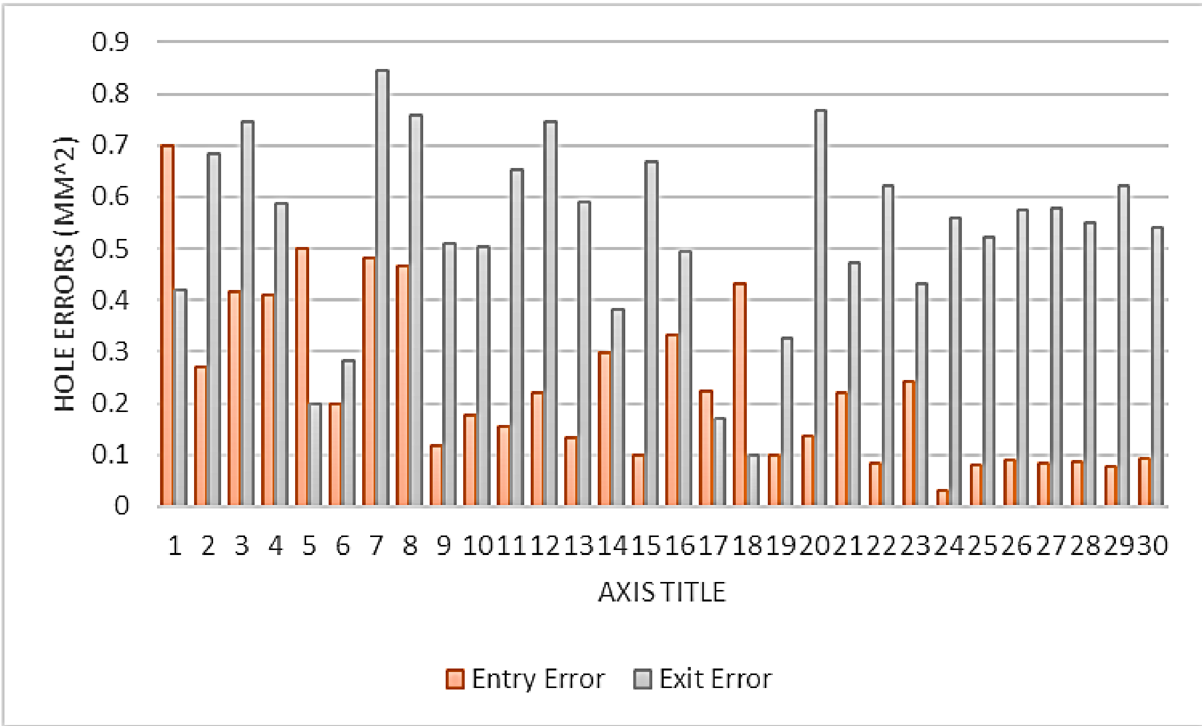

Figure 5. Hole error values for all runs.

Hole Entry		**Hole Exit**	
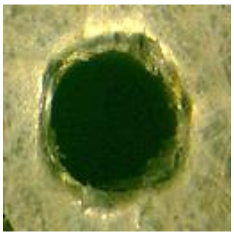	Run 16 Speed = 2500 rpm Feed rate = 0.1 mm/tooth Frequency = 27 KHz Amplitude = 3 µm Error = 0.032 mm^2	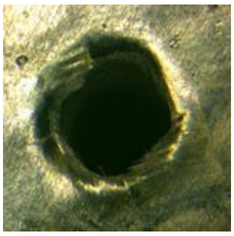	Run 18 Speed = 3000 rpm Feed rate = 0.075 mm/tooth Frequency = 23.5 KHz Amplitude = 2 µm Error = 0.099 mm2
Minimum Surface Error			
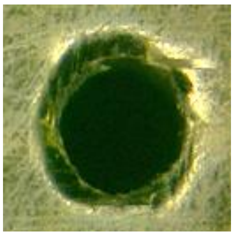	Run 1 Speed = 1500 rpm Feed rate = 0.05 mm/tooth Frequency = 20 KHz Amplitude = 1 µm Error = 0.699 mm2	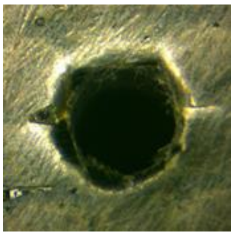	Run 7 Speed = 1500 rpm Feed rate = 0.1 mm/tooth Frequency = 27 KHz Amplitude = 3 µm Error = 0.845 mm2
Maximum Surface Error			

Figure 6. Sample for the minimum and maximum burr area formation.

Table 4 ANOVA for Hole Entry Surface Error

Source	Sum of Squares	DF	Mean Square	F Value	Prob > F
Model	0.61356	14	0.043826	3.565947	0.0100
A	0.001488	1	0.001488	0.121104	0.7327
B	0.002882	1	0.002882	0.234502	0.6352
C	0.00238	1	0.00238	0.193656	0.6662
D	0.225234	1	0.225234	18.32653	0.0007
A^2	0.184852	1	0.184852	15.04073	0.0015
B^2	0.023618	1	0.023618	1.921675	0.1859
C^2	0.039282	1	0.039282	3.196223	0.0940
D^2	0.032117	1	0.032117	2.613226	0.1268
AB	0.038123	1	0.038123	3.101899	0.0986
AC	0.009752	1	0.009752	0.79345	0.3871
AD	0.101602	1	0.101602	8.266962	0.0116
BC	0.006123	1	0.006123	0.498212	0.4911
BD	3.31E-05	1	3.31E-05	0.00269	0.9593
CD	0.007183	1	0.007183	0.58442	0.4564
Residual	0.184351	15	0.01229		
Lack of Fit	0.18418	10	0.018418	537.4895	< 0.0001
Pure Error	0.000171	5	3.43E-05		
Cor Total	0.797911	29			

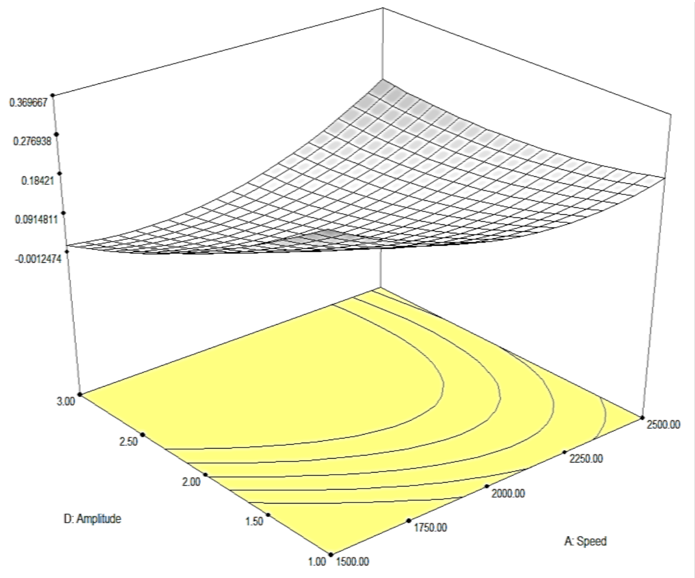

Figure 7. 3D response surface plot for hole entry error values.

The relationship between hole entry error value towards the RUAD parameters can be model in mathematical form and written as:

Hole Entry Error = 0.085 + 7.875E-3 A + 0.011B - 9.958E-3 C - 0.097D + 0.082A^2 + 0.029B^2 + 0.038C^2 + 0.034D^2 + 0.049AB + 0.025AC + 0.080AD + 0.020BC - 1.437E-3BD + 0.021CD

4.2 Effects of RUAD Parameters on Hole Exit Surface Error

Statistical ANOVA of exit surface error areas (Table 5) was performed to further investigated the effects of RUAD parameters. Based on the ANOVA, a quadratic model was selected to exemplify the cutting parameters effects towards the exit burr surface areas. From the analysis, it indicated that feed rate and spindle speed were the most significant factors that affect the hole exit accuracy. The results revealed that, with the increasing feed rate, the hole surface error value increased, which might due to the weakened anti-delamination effect of ultrasonic vibration in the drill process. On the other hand, the damage at the hole exit was mainly caused by the bending deformation of the uncut laminate due to the downward force action.

Figure 8 shows a 3d response surface plot on the entry burr area with regards to the speed and feed rate. Based on the graph, it shows that the minimum hole error surface occurred at the region when both feed rate and spindle speed are minimum.

The relationship between hole exit error value towards the RUAD parameters can be model in mathematical form and written as:

Hole Exit Error = 0.56 - 0.014A + 0.12B - 0.014C + 0.012D - 0.085A^2 + 0.018B^2 + 0.018C^2 + 5.573E-3 D^2 - 0.029AB -0.036AC - 0.025AD + 0.044BC - 0.048BD + 4.688E-3 CD

Table 5 ANOVA for Hole Exit Surface Error

Source	**Sum of Squares**	**DF**	**Mean Square**	**F Value**	**Prob > F**
Model	0.69967	14	0.049976	2.832715	0.0272
A	0.00462	1	0.00462	0.261888	0.6163
B	0.32877	1	0.32877	18.63502	0.0006
C	0.004401	1	0.004401	0.249455	0.6247
D	0.003337	1	0.003337	0.189147	0.6698
A2	0.196088	1	0.196088	11.11449	0.0045
B2	0.009083	1	0.009083	0.514854	0.4841
C2	0.009083	1	0.009083	0.514854	0.4841
D2	0.000852	1	0.000852	0.048284	0.8290
AB	0.013514	1	0.013514	0.765991	0.3953
AC	0.021243	1	0.021243	1.204078	0.2898
AD	0.009851	1	0.009851	0.55834	0.4665
BC	0.030888	1	0.030888	1.750766	0.2056
BD	0.037539	1	0.037539	2.127752	0.1653
CD	0.000352	1	0.000352	0.019927	0.8896
Residual	0.264639	15	0.017643		
Lack of Fit	0.258614	10	0.025861	21.46052	0.0017
Pure Error	0.006025	5	0.001205		
Cor Total	0.964309	29			

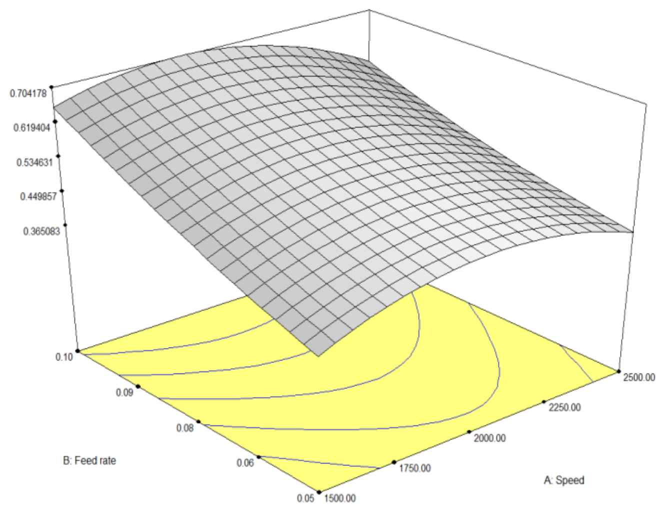

Figure 8. 3D response surface plot for hole exit error values.

5. CONCLUSION

With their unique and tailored enhanced properties, the usage of carbon fiber reinforced plastic (CFRP) laminate continues to growth while, at the same time, posture significant challenges in terms of poor machinability or specifically drilling process. It is evident that rotary ultrasonic assisted drilling can be as one of the alternative technique to increase the hole quality. Based on the conducted investigation, it shows that vibration amplitude and speed have significant effect for the hole entry surface error while feed rate and speed have significant effect for the hole exit surface error. The findings from the deliberately conducted experiments proved that careful selection of the rotary ultrasonic assisted drilling parameter is the key to achieving an economical and accurate drilling process for CFRP material.

ACKNOWLEDGEMENTS

The authors are grateful to the Malaysian Ministry of Higher Education and Universiti Teknikal Malaysia Melaka for their technical and financial support under Fundamental Research Grant Scheme No: FRGS/1/2012/FKP/F00477.

REFERENCES

[1] Kasim, M. S., Mohamad, W. N. F. W., Izamshah, R., Mohamad, N., Rosnan, H., Sundi, S. A., & Kasa, Z. M. Malaysian J. on Composites Sci. & Man., vol. **6** no. 1 (2021) pp. 1-13.

[2] SA, Sundi, R. Izamshah, and M. S. Kasim. Tribology Online, vol. **15**, no. 2 (2020) pp. 53-59.

[3] Z.C. Li, Y. Jiao, T.W. Deines, Z.J. Pei, C. Treadwell, Int. J. Mach. Tool Manufact., vol. **5** (2005), pp. 1402-1411

[4] Ding, H, Chen, SJ, Cheng, K., Proc. IMechE, Part B: J Engineering Manufacture, vol. **224** no. 12 (2010) pp. 1775–1783.

[5] Chern, GL, Chang, YC., Int. J. Mach. Tools Manufacture vol. **46** (2006) pp. 659–666.

[6] R. Izamshah, S.A. Suandi, M. Akmal, M. F. Jaafar, M.S. Kasim, S. Ding, Int. J. of Nanoelectronics and Materials, vol **13**, (2020) pp. 379-392.

[7] Ahmed, N, Mitrofanov, AV, Babitsky, VI. J Sound and Vibration vol. **308** (2007) pp. 845–854.

[8] Babitsky, VI, Mitrofanov, AV, Silberschmidt, VV., Ultrasonics vol. **42** (2004) pp. 81–86.

[9] Xiao, M, Sato, K, Karube, S., Int. J. Mach. Tools Manufacture vol. **43** (2003) pp. 1375–1382

[10] Azarhoushang, B., Tawakoli, T., Int. J. Adv. Manuf. Technol. vol. **57** (2011) pp. 945-955

[11] T. Tawakoli, B. Azarhoushang, Int. J. Mach. Tool Manufact., vol. **51** (2011), pp. 112-119

[12] K. Ding, Y. Fu, H. Su, F. Cui, Q. Li, W. Lei, H. Xu, Int. J. Adv. Manuf. Technol., vol. **91** (2017), pp. 3095-3105

[13] W.L. Cong, Z.J. Pei, C. Treadwell, Ultrasonics, vol. **54** (2014), pp. 1594-1602

[14] F. Makhdum, V.A. Phadnis, A. Roy, V.V. Silberschmidt, J. Sound Vib., vol. **333** (2014), pp. 5939-5952

[15] J. Pujana, A. Rivero, A. Celaya, L.N. López de Lacalle, Int. J. Mach. Tools Manuf., vol. **49** (2009), pp. 500-508